

Report of Evidence That Quantum Probability Is Itself Stochastic

Tim C Jenkins

Independent researcher

***Corresponding author**

Tim C Jenkins. Independent researcher

Submitted: 27 Aug 2022; **Accepted:** 05 Sep 2022; **Published:** 10 Sep 2022

Citation: Jenkins, T. C. (2022). Report of Evidence That Quantum Probability Is Itself Stochastic. *Adv Theo Comp Phy*, 5(3),560-564.

Abstract

This report covers work since a previous article on quantum probability. It provides evidence that quantum probability has a stochastic nature. This evidence is based on the number of electrons that need to be sent through a two-slit interferometer to gain a clear pattern of self-interference, which when compared with the number that would be expected to be sufficient in order for the position probability distribution of the self-interference wavefunction to take clear shape suggests that there is more variability present than that described by the formulation of quantum mechanics, which implies the presence of an underlying and as yet unrecognized physical process.

Keywords: Quantum Probability, Two-Slit Experiment, Self-Interference, Total Wavefunction, Simulation

Introduction

This is a report on a previous article [1] that presented a hypothesis that there is a stochastic archetype of quantum probability. That article noted an unexplained coincidence in quantum mechanics, namely that mathematically the interference term in the squared amplitude of superposed wavefunctions gives the squared amplitude the form of a variance of a sum of correlated random variables, not the form of a probability.

The article examined whether there could be an archetypal variable behind quantum probability that provides a mathematical foundation that observes both quantum and classic probability. The properties that would need to be satisfied for this to be the case were identified, and a generic hidden variable that satisfies them was found that would be present everywhere, transforming into a process-specific variable wherever a quantum process is active. Uncovering this variable confirmed the possibility that there is a stochastic archetype of quantum probability.

The aim now is to summarize the previous article and then provide practical experimental context for it by reporting work done since then in examining the quantum probability distribution involved in and the results of the famous 1989 experiment by Tonomura and colleagues that demonstrated the self-interference of electrons sent one by one through a two-slit interferometer, and by reporting the evidence found from this examination that supports the hypothesis of the previous article.

Key aspects of the previous article

The paradox

In the previous article the Schrödinger picture and the causal interpretation as recounted by Peter Holland in his quantum the-

ory of motion [2] were used, confined to a *single spatial dimension* to keep a focus on concepts. In one spatial dimension x the squared amplitude of the wavefunction is $|\psi(x,t)|^2 = \psi(x,t) \psi^*(x,t)$, where ψ^* is the complex conjugate of ψ , and the probability density $f(x, t)$ associated with the location of the particle being between x and $x + dx$ at time t is given by

$$f(x, t) = \frac{\psi(x,t)\psi^*(x,t)}{C(t)}$$

where $C(t)$ is a normalization constant $\int_{-\infty}^{\infty} \psi\psi^* dx$, which varies with t . Provided that $\int_{-\infty}^{\infty} \psi\psi^* dx$ is finite, $C(t)$ rescales the squared amplitude to a probability density by satisfying $\int_{-\infty}^{\infty} f(x,t)dx=1$ and reflects the fact that the particle exists somewhere at time t .

The one-dimensional Schrödinger equation is:

$$i\hbar \frac{\partial \psi}{\partial t} = \left(-\frac{\hbar^2}{2m} \frac{\partial^2 \psi}{\partial x^2} \right) + V\psi \tag{1}$$

where m is the inertial particle mass, $V=V(x,t)$ is the potential energy due to an external classic potential field, $\hbar = h/2\pi$, and h is Planck's constant. In this setup the superposition $\psi_{sum} = \psi_1 + \psi_2$ of two wavefunction solutions of equation (1) is also a solution of the Schrödinger equation, and calculating the squared amplitude of the superposition gives

$$R^2 = R_1^2 + R_2^2 + 2R_1 R_2 \cos \left[\frac{2\pi(S_1 - S_2)}{h} \right] \tag{2a}$$

The third term on the right describes the interference between the superposed waves, and its sign is variable depending on the phase difference [2]. Using the standard measure of h and expressing $\cos [2\pi(S_1 - S_2)/h]$ in the form $\cos (2\pi n + \theta)$, where n is an

integer and $0 \leq \theta \leq 2\pi$, then $\cos [2\pi(S_1 - S_2)/h] = \cos (2\pi n + \theta) = \cos \theta$ and equation (2a) simplifies to

$$R^2 = R_1^2 + R_2^2 + 2R_1 R_2 \cos \theta \quad (2b)$$

The remarkable feature of Equation (2b) is that the cosine is mathematically equivalent to and has all the attributes of a coefficient of correlation. Thus, from the standard result in statistics for the variance of the sum of two correlated random variables, the squared amplitude is mathematically equivalent to this variance, where the two variables have variance R_1^2 and R_2^2 and a correlation coefficient of $\cos \theta$.

The approach taken

The starting point taken in the previous article to resolve the paradox was to suppose that before normalization, the squared amplitude is associated with a hidden variable whose mean equals the variance of another closely related and relevant hidden variable, a property called there the mean/variance property. Finding a pair of such variables with the properties needed to be consistent with quantum mechanics was the purpose of the previous article. The generic forms of such variables were called the unit base variable and the unit squared amplitude variable, respectively, with the unit base variable having a mean of zero and variance of one, and the unit squared amplitude variable being the square of the unit base variable in order that its mean equals 1, the variance of the unit base variable (the mean/variance property).

The element of a wavefunction that is directly relevant to equation (2b) and capable of having these properties is its real part, the product of its amplitude and the cosine of its argument, which captures its essence. Accordingly, it was proposed that the unit base variable may be the product of two independent variables, an amplitude variable, and a cosine variable, and the unit squared amplitude variable and the related unit base variable would form the pair being searched for.

The search for these variables led to:

1. A generic variable Z which is the square of another generic variable W , which is the product of two independent seed variables A and C :
 - a. Variable $A \sim U(0,3)$, which is a generic stochastic analogue of the amplitude of a wavefunction, and
 - b. Variable $C \sim U(-1,1)$, which is a generic stochastic analogue of the cosine of the argument of a wave function.
2. The dependent unit base variable W is the zero mean/unit variance generic stochastic analogue of the real part of a wavefunction, properties that come from the supports of A and C .
3. The dependent unit squared amplitude variable Z is the unit mean generic stochastic analogue of the square of the real part of a wavefunction.

When and where a quantum process is active, the unit generic variables W and Z were hypothesized to become i.i.d at each such point and time (x, t) , instantaneously transforming through scaling by a scale factor (SF) into specific stochastic processes. In the case of W , SF is the square root of the the deterministic squared amplitude of the specific quantum process that is ac-

tive there and then, and in the case of Z , SF is that deterministic squared amplitude. The probability density and cumulative density functions of W and Z and of the transformed scaled variables which were denoted X and Y respectively were then derived.

The generic variables that culminate in the unit squared amplitude variable Z are not linked to any point in space or time. It seems that Z describes a regular simultaneous vibration-like phenomenon throughout the universe, effectively a universal clock in which the intensity of the phenomenon varies randomly from instant to instant, with points on the support of Z , $0 < z \leq 9$ being in correspondence with this intensity. In each instant this generic variable was formulated to be simultaneously transformed across the universal set of active quantum processes, wherever and for as long as a process is active, into a corresponding universal set of process-specific squared amplitude variables and their stochastic processes. This transformation involves the generic universal variable Z becoming a set of independent and identically distributed variables spanning each spatial point and time at which a quantum process is active (but remaining generic and universal elsewhere), with the realization of the variable at a point being scaled by SF , the deterministic squared amplitude of the specific quantum process that is active there.

The crux of the previous article

In short, the previous article presented a formulation in which behind the squared amplitude of either a superposed or individual wavefunction as formulated in the causal interpretation, there could be an associated specific variable Y at each applicable point in space and time that originates from a universal generic archetypical variable Z .

The variable Y has a mean at each point and time that equals, and whose average realization over repeated trials of an experiment converges to, the deterministic squared amplitude. When the counts of realizations at each point and time are normalized to their relative frequencies, their averages converge with repeated trials to the set of probabilities predicted by the causal interpretation of quantum mechanics that the particle whose motion is described by its wavefunction is at these points.

Importantly, the article showed that despite being developed using classic probability theory, the variable Y and its stochastic process can relate to either a local or a nonlocal quantum mechanical process.

The normalized squared amplitude in the two-slit interferometer experiment

The setup

The setup for a two-slit interferometer experiment follows Holland [3] which in turn follows Philippidis et al [4]. Electrons are sent one at a time from a source through a two-slit barrier and detected at a screen. The direction from the source perpendicular to the screen is the x axis of a two-dimensional coordinate system with origin 0 where the x axis meets the barrier, and the y axis is the other one. The slits are denoted B and B' and their centres are at the points $(0, \pm Y)$. The wave incident on the slits is taken to be plane, $\psi = ae^{i(k_1 x + k_2 y)}$ where a is a constant and $u_1 = \hbar k_1 / m$ and $u_2 = \hbar k_2 / m$ are the x and y components of velocity and k_1, k_2 are the reciprocals of the wavelengths in the respective x and y

directions. It is assumed that two Gaussian wave packets are formed at the slits and that the instant when this happens is time zero, $t=0$. The packets move with relative group velocity $2u_2$ and spread into one another, with interference coming from both relative motion and dispersion [5].

Holland gives [5] the wavefunctions of the two packets $\psi_B(x,y,t), \psi_{B'}(x,y,t)$ and the total wavefunction $\psi(x,y,t)=N[\psi_B(x,y,t)+\psi_{B'}(x,y,t)]$, where $N=(2+2e^{-Y^2/2\sigma_0^2})^{-1/2}$ is the normalization constant of the total wavefunction, and σ_0 is the rms at each slit [6]. Our interest is in the probability distribution of the electron position in the y dimension, which is considered next.

The squared amplitude and its parameters

Holland gives the normalized squared amplitude of the total wavefunction to be [7]:

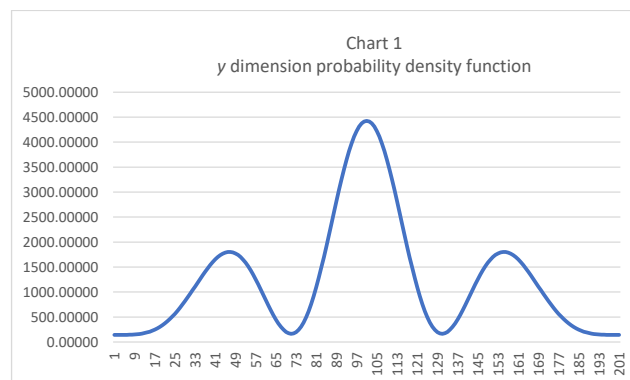
$$\langle R^2(y,t) = a^2 N^2 (2\pi\sigma^2)^{-1/2} e^{-[y^2+(Y+u_2t)^2]/2\sigma^2} \text{ times } \{e^{y(Y+u_2t)/\sigma^2} + e^{-y(Y+u_2t)/\sigma^2} + 2\cos[2k_2y - (Y+u_2t)y\hbar t/2m\sigma_0^2\sigma^2]\}, \text{ where } \sigma = \sigma_0[1 + (\frac{\hbar t}{2m\sigma_0^2})^2]^{1/2} \text{ [6]} \quad (3)$$

We will now study the probability distribution in a case where the screen is 35cm behind the slits. The parameters adopted are informed from Holland [8], who based them on actual experiments [9], and are as follows:

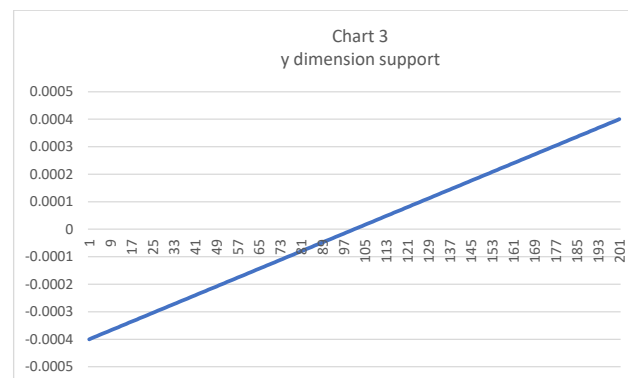
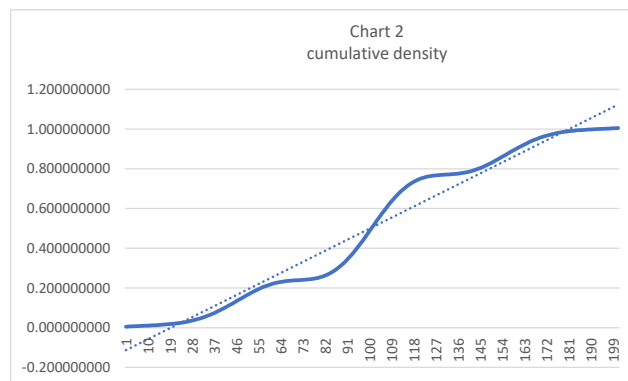
$u_1=1.3x10^{10} \text{ cm s}^{-1}$, $u_2=1.5x10^4 \text{ cm s}^{-1}$, $\sigma_0=10^{-5} \text{ cm}$, $Y=5x10^{-5} \text{ cm}$, with $(m=9.11x10^{-28} \text{ g}, \hbar=1.055x10^{-27} \text{ g cm}^2 \text{ s}^{-1})$, and $t=2.7x10^{-9} \text{ s}$, the latter because $x=u_1 t$, and the x-component of an electron reaches the screen 35cm beyond the origin at the interferometer at $t=x/u_1=2.7x10^{-9}$ seconds.

From the expression in the previous subsection $N=0.707105464$ and in conjunction with it the plane wave constant a is set to 1.0133279 to achieve a numerically calculated cumulative probability density equal to one at $y = .0004 \text{ cm}$, the righthand end of the probability support, which in this setup is $-.0004 \text{ cm} \leq y \leq .0004 \text{ cm}$, with the range of .0008 cm representing the detection width.

The pdf has a mean $\mu=0$ and using [6] a standard deviation $\sigma=1.56659x10^{-4}$ and is shown in Chart 1, which clearly shows a pattern of multiple probability peaks and troughs. These will translate, as the cumulative number of electrons sent through the interferometer increases, into increasingly distinct bands of dense detection separated by sparse detection with varying detection density within the bands from peak to trough, and vice versa, taking shape across the entire detection screen. The cumulative density function of this distribution and its trendline are shown in Chart 2, and Chart 3 gives the values of y at each numbered point. The difference between each of the 201 points is 0.000004 cm, with every eighth of the 201 points in the support of the distribution, including end points being shown. y ranges from $-.0004$ to $.0004$ and is zero at point 101, where the pdf is at its maximum.



Note: For continuous random variables the probability that the variable takes on any particular value is 0, and it is of course common for pdf values to exceed one.



Evidence that quantum probability is itself stochastic

At this point the aim would usually be to simulate equation (3) and compare the results with those obtained experimentally using a setup for which the parameters described above are suitable. However, the probability distribution described by equation (3) does not lend itself to simulation, nor are the parameters necessarily suitable for every setup, and it is necessary to adopt an alternative approach. Fortunately, the celebrated experiment performed by Tonomura [10], in particular Figure 2 from the paper that is reproduced below, provide such an alternative.

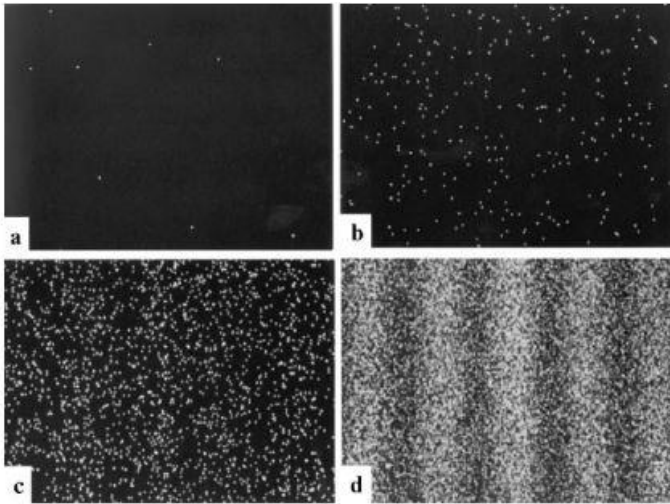
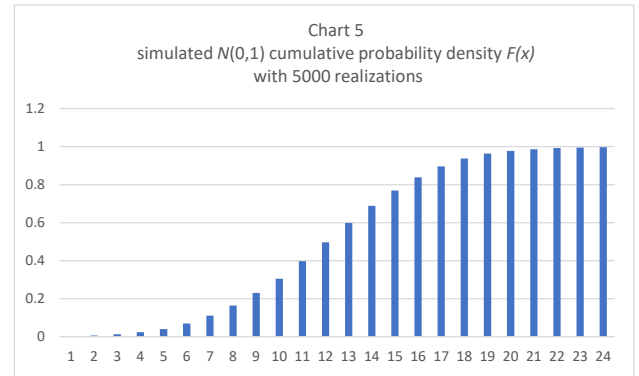
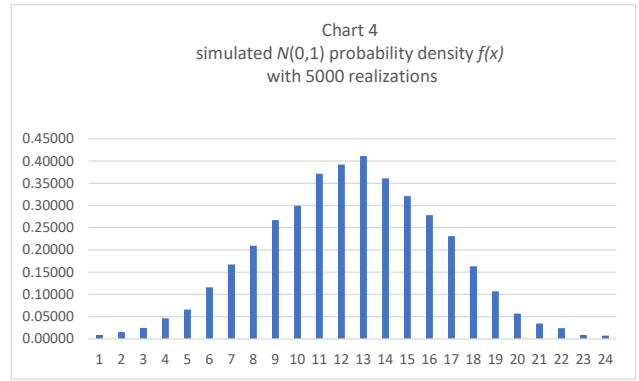


Figure: Buildup process of electron interference pattern. Number of electrons: (a) 8; (b) 200; (c) 6,000; (d) 140,000.

This figure acts as the experimental equivalent of a simulation, illustrating the number of electrons (140,000) that needed to be emitted in order for the relatively clear image (d in Fig. 2) of self-interference to have formed on the detection screen of the interferometer, with the central bands showing a pattern of detection density akin to that given by the probability density function shown in Chart 1 and described by equation (3). Adopting a set of parameters that describe the setup in the Tonomura experiment and plugging them into equation (3) should yield a probability distribution similar to that in Chart 1 and specific to the Tonomura experiment.

The number of realizations needed to clearly simulate a distribution

However, before discussing this further, we turn to a simulation of the probability density $f(x)$ and cumulative density $F(x)$ of the standard normal distribution to see how many realizations are needed for a relatively clear picture of these distributions to emerge. The result of 5000 realizations of the pdf is shown in Chart 4 and of the cdf in Chart 5. The difference between each of the 24 points in the charts is .25, creating 24 bins in which the values from 5000 realizations using the Excel function NORMINV(RAND(),0,1) are counted, according to which bin their value falls, in a similar fashion to that described in Appendix C of the previous article (but see the caveat below), and with x ranging from -3 to 3.



These counts are then expressed as relative frequencies by dividing by 5000 to get the increase in the cdf in a bin and in the case of the pdf by multiplying the relative frequencies by 4 to allow, as explained below, for the fact that $f(x) = d/dx F(x)$. The resulting simulated $f(x)$ values span a range from -.0040 to .0056 with a peak of .4 when $x=0$, and the corresponding $F(x)$ values range from .0022 to .9968. These charts give a relatively sharp picture of the standard normal distribution.

The reason that the factor 4 that is applied to the relative frequencies of bin counts to arrive at the pdf is that using the standard normal distribution the expected number of realizations in a bin beginning at x and ending at $x+.25$ is $5000(F(x+.25)-F(x))$ and the average rate of change in the cdf over the range of the bin is $((F(x+.25)-F(x))/.25)$, making 4 times the relative frequency of the bin count the simulated average value of $f(x)$ within the range of the bin.

[Caveat: The notation at the end of Appendix C in the previous article has caused some confusion. To be clear the reference there to a bin ranging from SF to 1.25SF means the bin from 1 to 1.25 for the relevant SF, and likewise the cdf interval in the term $5000(F(1.25SF) - F(SF))$ that follows means the cdf at 1.25 for the relevant SF minus the cdf at 1 for that SF]

The significance of this exercise is that if 5000 realizations of a simulated standard normal variable are sufficient to provide a relatively clear picture of its distribution then, provided that a degree of relative, rather than absolute, clarity is acceptable, 5000 simulations are also enough to do the same for any other distribution where the probability distribution and the parameters it employs are known [11], including the interference distribution described by equation (3) with parameters that describe the setup in the Tonomura experiment. Why then does it take

140,000 electron emissions through a two-slit interferometer to gain a relatively clear picture of the self-interference effect?

Conclusion - the answer to this question

It is suggested that the answer to the question above is that the nature of probability in quantum mechanics is not solely determined by the normalized squared amplitude of the wavefunction of a quantum mechanical process, but rather originates from a random variable whose mean equals that deterministic squared amplitude. The resulting variability around the mean would lead to a much larger number than the otherwise sufficient 5000 or so electron emissions to be necessary for a relatively clear picture to form, as happened in the Tonomura experiment, and for the average of the realizations of the squared amplitude variable at a point and time (x, t) to converge to the deterministic squared amplitude as it is formulated in the causal interpretation of quantum mechanics.

This suggestion is of course only a mathematical one which, if valid, would be the manifestation of some underlying and as yet unrecognized physical process that introduces more variability into quantum probability than is described in the existing formulation of quantum mechanics. Regrettably, it is beyond the scope of this report and outside the field of its author to speculate on what such a process might be.

References

1. Tim C Jenkins. (2021). A Search for A Stochastic Archetype of Quantum Probability. *Adv Theo Comp Phy*, 4(4), 304-313.
2. Holland, P. R. (1995). *The quantum theory of motion: an account of the de Broglie-Bohm causal interpretation of quantum mechanics*. Cambridge university press.
3. *ibid*, p176.
4. Philippidis, C., Dewdney, C., & Hiley, B. J. (1979). Quantum interference and the quantum potential. *II Nuovo Cimento B* (1971-1996), 52(1), 15-28.
5. P.R. Holland, *The Quantum Theory of Motion: an account of the de Broglie-Bohm causal interpretation of quantum mechanics*, vol. Paperback (Cambridge University Press, Cambridge, (1997), p 177
6. *ibid*, pp 158-159.
7. *ibid*, p 178.
8. *ibid*, p 179.
9. C. Jönsson, *Z. Phys.*, 161, pp 454-474.
10. Tonomura, A. (2008). Development of electron holography and its applications to fundamental problems in physics. *Japanese journal of applied physics*, 47(1R), 11.
11. Lerche, I., & Mudford, B. S. (2005). How many monte carlo simulations does one need to do? II. Lognormal, binomial, cauchy, and exponential distributions. *Energy exploration & exploitation*, 23(6), 429-461.

Copyright: ©2022 Tim C Jenkins. This is an open-access article distributed under the terms of the Creative Commons Attribution License, which permits unrestricted use, distribution, and reproduction in any medium, provided the original author and source are credited.